

# Delineation of Frost Characteristics on Cold Walls by Using a New Formula for Psychrometrics Demarcation Boundary

Ahmed Hamza H. Ali\*

*Department of Mechanical Engineering, Faculty of Engineering, Assiut University, Assiut 71516, Egypt*

## Abstract

In this study, a direct new formula that predicts frost formation on cold walls corresponding to psychrometric-sub-saturated. The new formula uses data of the entering air dry-bulb temperature and absolute humidity and absolute humidity of air at saturation corresponding to the coil surface temperature. To validate the formula, case studies of demarcation criteria for frost formation on evaporator coil using experimental measured data and on walls of cold storage freezer using measured data from literature are used. Results completely match with the graphic plot of the data on the psychrometric chart. In case of cold storage freezers, results clearly show that a greater demarcation criteria value indicates frost formation under severe condition, as snow-like with low density and thermal conductivity.

© 2008 Jordan Journal of Mechanical and Industrial Engineering. All rights reserved

*Keywords:* frost formation; psychrometric-sub-saturated; demarcation criteri; and Psychrometric-Supersaturated Region

## Nomenclature

### Alphabetic symbols

a, b and c: coefficient in equation 2  
D : demarcation condition,-\*  
P : partial pressure, Pa  
P : total pressure, Pa.  
RH: relative humidity, %  
T : temperature, Co  
UA: total conductivity, W/ oC.  
W : humidity ratio, kgH<sub>2</sub>O/kgda

### Subscripts

a: air  
cs: coil surface  
  
critical: critical  
da : dry air  
DB : dry bulb  
Dry : dry  
Fr : frost  
H<sub>2</sub>O : water vapor  
Ice : ice  
In : entering  
Load : load  
Out : leaving  
Ref : refrigerant  
S : saturation  
Scw : supercooled water  
Sw : saturated water

## 1. Introduction

Frost problems often occur in cold storage freezers because of infiltration of warm humid air through access doors. When the cold storage freezer door open, air at the upper layers in the docks rushes inside freezer in order to replace ex-filtrated air and it mixes with freezer air in the upper layers of the freezer. This air mixture creates fog and ice fog crystals that deposit on the freezer walls and products. Also, as moist air is cooled by passing over evaporator coil that has surface temperature below both dew point and freezing point of the air, near the coil surface, frost forms and deposits on the coil surface. The word frost in this study refers to the formation of ice crystals in air or on surfaces, either by freezing of a dew droplet or by a phase change from water vapor to ice directly. Frost deposition on the walls of cold storage freezers and evaporator coil is usually undesirable. The main problems associated with frost growth on an evaporator coil are the decline in heat exchanger efficiency resulting from an insulating effect of the frost layer and the rising pressure drop due to a decreasing hydraulic diameter of the flow channel, which increases the energy consumption of the air-blowing fan. Whereas, in cold storage freezers, products quality suffers as frost forms on products in the freezer. For these reasons frost must be removed be means of defrost for restoring coil performance or to be removed away manually form the walls and products in cold storage freezers. The physical structure of frost layer forming on an evaporator coil depends on many factors, including the evaporator coil design and its operating temperature, entering air dry-bulb

\* Corresponding author.e-mail: ah-hamza@aun.edu.eg.

temperature and relative humidity, and face velocity of air entering the coil, Şahin [1]. Dietenberger [2] characterizes the first regime of frost formation over cold wall as follows: the initial frost layer can begin in one of two ways. In the first case, initial condensation occurs at nucleation sites on the wall resulting from a critical supersaturation. In the other case (i.e. for a very cold wall), boundary layer fogging occurs, and fog becomes the major source for water droplet condensation on the wall. For cooling of moist air at freezer temperatures, Smith [3] proposes a concept of frost formation in accordance with a graphic plot on a psychrometric chart. The concept suggests that when the line representing temperature and absolute humidity of the air cross saturation curve of the psychrometric chart (i.e., become supersaturated), the unfavorable frost formation occurs.

Once a supersaturated state exists in air, whose temperature is below freezing point, fog and ice fog are likely to form, based on operating temperatures. This formed frost under supersaturated condition has affinity to deposit on any surface in their path inside the freezer. When it is deposited over evaporator coil, it has higher impact on reduction of coil airflow rate, and it needs more energy to defrost than frost formed under less extreme conditions do.

A symptom of such frost when formed on evaporator coil is that the coil performance deteriorates rapidly and coils seemingly require near-continuous defrosting. Smith [4 and 5] discusses his concept [3] of applied psychrometrics in typical industrial freezers issues pertaining to latent heat - equipment-related loads. Sherif et al. [6], Mago and Sherif [7], and, Cleland and O'Hagan [8] experimentally confirm Smith's concept [3] by using real size evaporator coil.

Throughout the literature, it is evident that few researches (Smith, Sherif and coworkers, and, Cleland and coworkers) investigate demarcation boundary of frost formation inside cold storage freezers or real size evaporator coil, either in subsaturated or supersaturated regions with the aid of the psychrometric chart. In addition, Cleland and O'Hagan [8] publish the only available formula in literature, for delineation of the demarcation criteria that declare whether frost is formed in supersaturated and subsaturated regions, based on Smith [3] concept. They use the definition of a critical load sensible heat ratio (SHR), and they report that if the actual heat loads have a SHR, less than the critical value, then unfavorable frost will be expected to occur. Cleland [9 and 10] uses this demarcation criterion to explore aspects of refrigerated facility design and operation, and to consider the effect of infiltration air into a frozen warehouse and loading dock, respectively. Cleland and O'Hagan [8] report that data used is not of sufficient quality either to fully prove or disprove proposed transition between frost types.

For cold storage freezers, prediction of frost formation type guides refrigerating system designers in their quest for improved designs and efficient operation. Therefore, in this study, a direct formula predicting demarcation

boundaries in psychrometric saturation of delineation frost formation on cold walls is presented. It indicates if frost is formed in psychrometric-sub saturated or supersaturated regions. The formula uses data of the entering air dry-bulb temperature, absolute humidity, and the absolute humidity of air at saturation correspondence to the coil surface temperature. Case studies from experimental measurements, as well as measured data from literature, are used to validate the formula. Subsequently, characteristics of frost formed on the cold walls for the studied cases are described.

## 2. Analysis

The following premises are applied on psychrometric chart too formulate the demarcation boundaries in psychrometric chart in order to declare whether frost formed in psychrometric-sub saturated or supersaturated regions, and to delineate the frost type formed on cold walls, using Smith (1989) concept, a straight-line path describing air-cooling process, line (C-D) in subsaturation or line (A-D) in supersaturated case as shown in Figure 1; and is plotted on the psychrometric chart. The beginning of the path line is the entering air condition, while the end-point of the path line is coil surface temperature or cold storage freezer temperature; and lies on the psychrometric saturation curve. In this step, straight-line approximation approach of Stoecker [11] and ASHRAE [12] - for cooling and dehumidification through a coil that relates the change in conditions of the air passing the cooling coil- is used.

Demarcation from subsaturated to supersaturated regions, critical condition, and lay at minimum coil refrigeration temperature correspond to the lowest coil surface temperature, which can occur without causing straight-line path to invade the supersaturated region of the chart. In the premise, line (B-D) in Figure 1 is plotted tangential to the psychrometric saturation curve at the coil surface temperature or cold storage freezer temperature.

If the air path invades the supersaturated region, the case of line (A-D) in Figure 1, frost precipitation occurs within the airstreams, and it deposits on cold walls in their path. Where the path does not invade the supersaturated region (e.g. the case of line C-D in Figure 1), the coil-frost is of ice-like quality, and formed over the cold walls.

The following points should be addressed with the premises plotted in Figure 1. The refrigerant evaporation temperature,  $T_{ref}$ , can be occasionally used instead of coil surface temperature,  $T_{cs}$  (i.e. point D' in Figure 1). Indeed, using ( $T_{ref}$ ) represents a minimum border for  $T_{cs}$ , and will lead to conservative estimates of the demarcation boundaries as frost is formed in the supersaturation region. Another point is that in case of evaporator coil - as the time passes frost layer thickness increases- frost surface temperature increases. It should be used as the end-point of the straight-line approach on psychrometric saturation curve, point D" in Figure 1. In this case, the condition for frost formation shifts the demarcation boundaries slightly into subsaturated region.

To alter the graphic concept into a formula, an equation is required to relate air absolute humidity at saturation condition with air dry-bulb temperature and psychrometrics saturation curve. The absolute humidity at saturation,  $W_s(T_a)$ , as function of the air dry-bulb temperature is calculated from ASHRAE [13] by:

$$W_s(T_a) = 0.622 \left( \frac{p_s(T_a)}{P_a - p_s(T_a)} \right) \quad (1)$$

Where  $P_a$  is total static pressure of the air in Pa, and  $p_s(T_a)$  is the saturation vapor pressure in Pa as a function of air dry-bulb temperature,  $T_a$ , in °C. Magnus [14] equation, which is the fit to the Clausius–Clapeyron equation for  $p_s(T_a)$  is used in this study and is given by

$$p_s(T_a) = a \exp\left(\frac{bT_a}{c + T_a}\right) \quad (2)$$

The coefficients a, b and c are set, and they are obtained from correlation of measured data. Magnus [14] equation is the most widely used approximation for calculation of  $p_s(T_a)$  in terms of accuracy and usability in analytical expressions.

In the literature, there are different set of coefficients for Magnus equation.

In this study, selection of such set is based on the deviations between the tabulated values in ASHRAE [13] for absolute humidity at saturation with correspondence values calculated by a set of coefficients using eqs. (1 and 2).

Set of coefficients obtained from Magnus [14], Sonntag [15], WMO [16], and Whiteman et al. [17]. Their validity temperature range are presented in Tables (1 and 2) for both saturation vapor pressure with water and ice, respectively. The calculated correspondences of deviation values to each set at certain temperature range are also shown in last rows of Tables (1 and 2). As Table 1 shows, for absolute humidity at saturation with water, the minimum deviation is obtained when using Whiteman *et al.* [17] set of coefficients.

As Table 1 shows, for absolute humidity at saturation with ice, the minimum deviations are obtained by using either WMO [16] or Whiteman *et al.* [17] sets of coefficients; and are almost equal.

Only, Whiteman *et al.* [17] presents an extra set of coefficients for saturation vapor pressure with super

cooled water, the case of fog in supersaturated region. Therefore, the set of coefficients of Whiteman et al. [17] shown in Table 3 for the cases of saturation vapor pressure over water, super cooled water, and ice will be used in this study.

To calculate the demarcation boundaries that define whether the frost is formed in psychrometric subsaturated or supersaturated regions in psychrometrics saturation, the tangent line (B-D) in Figure 1, and the slope of approach line (B-D) to the psychrometric saturation curve equal the differentiation of equation 1. For this purpose, equation 1 is approximated by:

$$W_s(T_a) \approx 0.622 \left( \frac{p_s(T_a)}{P_a} \right) \quad (3)$$

The deviations among tabulated values in ASHRAE [13] for the absolute humidity at saturation with correspondence values were calculated using equation 3 in the temperature range from -40 to 0 °C is ranged from 0.552% to 0.991%. While, that was calculated with equation 1 as shown in Table 2. A set of coefficients of Whiteman et al. [17] ranged from 0.47% to 0.6%. Therefore, a less complicated formula of the critical demarcation boundary and the slope of the line (B-D) in Figure 1 is the differential of equation 3 at the coil surface temperature,  $T_{sc}$ , in °C is given by:

Table 1: Coefficients of equation 2 for saturated vapor pressure over water and deviations of  $W_s$  with ASHRAE [13] values.

	Magnus [14]	Sonntag [15]	WMO [16]	White man et al. [17]
a	603.7074	611.213	611.2	610.78
b	17.1485	17.5043	17.62	17.0809
c	234.69	241.2	243.12	234.175
Valid in $T_a$ range	-20 to 118 °C	-30 to 70 °C	-45 to 60 °C	-60 to 20 °C
$\frac{W_{s,ASHRAE} - W_s}{W_{s,ASHRAE}}$	1.2% to 1.6%	0.38% to	0.38% to	0.26% to 0.44%
( $T_a$ range 0 to 20 °C)		0.59%	0.69%	

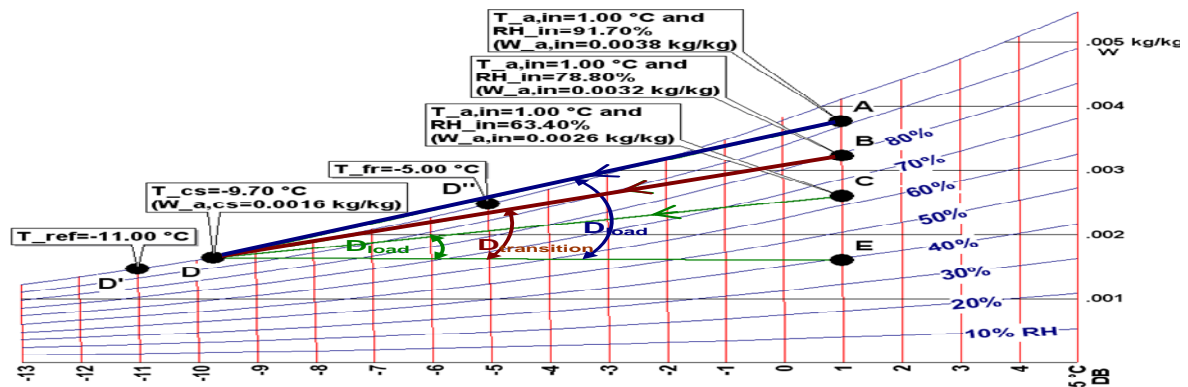


Figure 1 : Psychrometric plot of the demarcation criteria principles used to in this study.

TABLE 2: Coefficients of equation 2 for saturated vapor pressure over ice and deviations of  $W_s$  with ASHRAE [13] values.

	Sonntag [15]	WMO [16]	Whiteman et al. [17]
a	611.213	611.2	610.71
b	17.5043	22.46	22.4429
c	241.2	272.62	272.44
Valid in $T_a$ range	-60 to 0.01°C	-65 to 0°C	-60 to 0°C
$\frac{W_{s,ASHRAE}-W_s}{W_{s,ASHRAE}}$	0.4%	0.39%	0.47%
$W_{s,ASHRAE}$	to	to	to
( $T_a$ range -40 to 0°C)	0.96%	0.52%	0.6%

TABLE 3: The coefficients used in this study for equation 2 from Whiteman et al. [17].

For saturation vapor pressure	a	b	C
over water	610.78	17.0809	234.175
over supercooled water	610.78	17.8436	245.425
over ice	610.71	22.4429	272.440

$$D_{\text{critical}} = \frac{\partial W_s(T)}{\partial T} = a \left( \frac{0.622}{P} \right) \left( \frac{b}{T_{cs} + c} - \frac{bT}{(T_{cs} + c)^2} \right) \exp \left( \frac{bT}{T_{cs} + c} \right) \quad (4)$$

While the While the slope of the load line, either (C-D) or (A-D), is shown in Figure 1 and can be calculated by:

$$D_{\text{load}} = \frac{W_{a,\text{in}} - W_s(T_{cs})}{T_{a,\text{in}} - T_{cs}} \quad (5)$$

Where  $W_{a,\text{in}}$  is the absolute humidity of the air entering the coil. And  $T_{a,\text{in}}$  and  $T_{cs}$  are the entering air dry-bulb temperature. And the coil surface temperature is approximated, in some cases, by the refrigerant evaporation temperature, respectively.

The Ratio of the slope of the load line,  $D_{\text{load}}$ , to the slope of the critical demarcation line,  $D_{\text{critical}}$ , is the criteria used in this study defining the demarcation boundaries that clarify whether the frost is formed in psychrometric-subaturated or supersaturated regions. The Ratio is given by:

$$\text{Ratio} = \frac{D_{\text{load}}}{D_{\text{critical}}} \quad (6)$$

If the value of the Ratio is greater than 1.0, the load approach line is crossing the psychrometric saturation curve, and, in this case, frost is formed under supersaturation condition. Thus, as the air temperature falls below its dew point, it is possible for fog droplets to be nucleated, and ice fog is likely to form based on operating temperatures. If the value of the Ratio < 1.0, the load approach line is completely in the psychrometric

subaturated region, and the formed frost on the cold walls is of ice-like quality.

### 3. Experimental Measurements

The test apparatus, experimental procedure, and data reduction techniques described in Ali and Ismail [18] are used to investigate the effect of frost formation on the evaporator coil in psychrometric-subaturated region with minor modifications in the apparatus. The modifications are increasing the capillary tube length, and are cooling the last eight tubes in the condenser by water. However, with this apparatus and indoor environmental conditions, frost formation on the coil surface occurs at a face velocity of 0.612 m/s or less. The measurements were performed at the Heat Laboratory, Assiut University, Egypt.

### 4. Results and Discussion

Experimental measurements, as well as measured data from literature, are used to validate the formula for the demarcation criterion in cases of frost formation on the evaporator coil, and on the walls in cold storage freezer. Furthermore, the characteristic of the formed frost under this condition is described.

#### 4.1. Frost Formation on the Evaporator Coil in Psychrometric-Subaturated Region and its Characteristics

To validate the criterion of the demarcation boundaries presented in this study that declare whether the frost is formed on the coil in psychrometric-subaturated or supersaturated regions and characteristics as well, an experiment was carried out at a higher freezing temperature with face velocity of 0.612 m/s for a number of hours. The operating conditions for this experiment, as well as the experimentally determined coil performance in terms of the ratio of the coil total conductivity (UA) under frost to dry conditions, is shown in Figure 2. The performance results shown in the figure indicate that at early stage of frost formation on the coil, the determined ratio of total conductivity at thin frost layer formation to dry coil condition, ( $UA_{\text{fr}}/UA_{\text{dry}}$ ) for the presented operating conditions is 1.1. At 2.25 hours later. The frost layer thickness is increased, and consequently the ratio ( $UA_{\text{fr}}/UA_{\text{dry}}$ ) is decreased to 0.86. To interpret these results, the demarcation criterion is applied to the operating condition correspondence to the points giving ratios ( $UA_{\text{fr}}/UA_{\text{dry}}$ ) of 1.1 and 0.86, as shown in Figure 2 at time = 0 and 2.25 hours respectively. The plot of the operating point condition at time zero on psychrometric chart shown in Figure 3 are the points (A-A'-A''). whereas the condition at time=2.25h are points (B-B'-B''), respectively. The calculated criteria value correspondence to points (A-A'-A'') is (Ratio) 0.84, while for points (B-B'-B'') is 0.83, respectively. Comparing calculated criteria with plotted data on the psychrometric chart of Figure 3 indicates that they are completely matched. Clearly, with these calculated and plotted demarcation criterion values, the frost is formed on the coil during this experiment in psychrometric-subaturated region. A photograph showing the formed frost on the coil face under this condition is

also shown in the Figure 3. A close visual examination of the nature of frost formed on the coil under the aforementioned condition was found to be thin, fluffy, and dryer. This declares that the type and shape of frost crystal forms on the coil surface reflect its growth environment. Interpretation of the performance results as the ratio ( $UA_{fr}/UA_{dry}$ ) was 1.1 in early stage of frost formation; and became 0.84 as frost thickness increases is explained as follows.

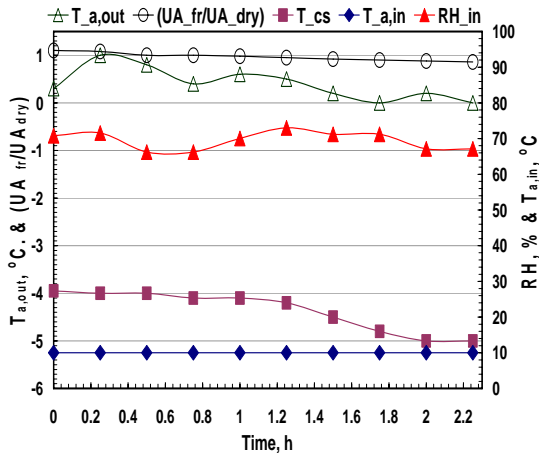


Figure 2 : Effect of formed frost at higher freezer temperature correspondence to psychrometric-sub-saturated region on evaporator coil performance.

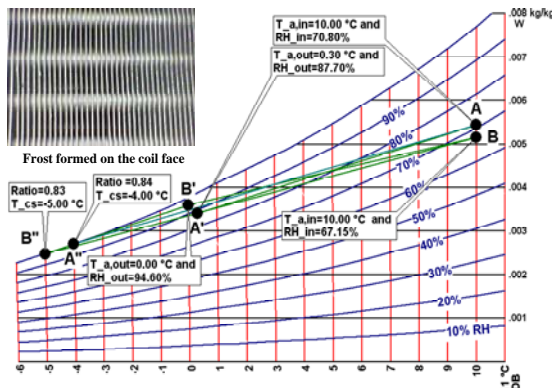


Figure 3 : Psychrometric plot of measured data to declare the demarcation criteria conditions.

For coil surface temperature range from 0 to  $-4^{\circ}\text{C}$ . And a condition of frost formation on the coil surface exists in psychrometric-sub-saturated region. Under this operating condition, air temperature in near wall boundary is cold; and is having very small size moisture droplets. As these small droplets settled on the cold coil surface, it results in a formation of very light fluffy ice crystal shape made up of six sided individual ice crystals (plates) - based on Libbrecht [19] morphology diagram. These formed individual thin crystals (plates) create roughness over the coil surface that leads to this enhancement in the heat transfer coefficient i.e. the mass transfer coefficient. Moreover, a thin frost layer covering the coil surface leads to a higher driving force for mass transfer between mist

droplets in the boundary layer and frost surface. The driving force is the vapor pressure difference over mist droplets and outer surface of the formed frost. This driving force is starting to exist with frost formation, see Figure 4. Figure 4 is a plot of vapor pressure difference of water (mist in subsaturated region), ice, vapor pressure difference of super cooled water (fog in supersaturated region), and ice. The pressure differences are calculated from equation 2 using the set of coefficients from Table 3. Due to the crystalline structure of ice, water molecules are not able to break free from an ice surface as easily as from a water surface.

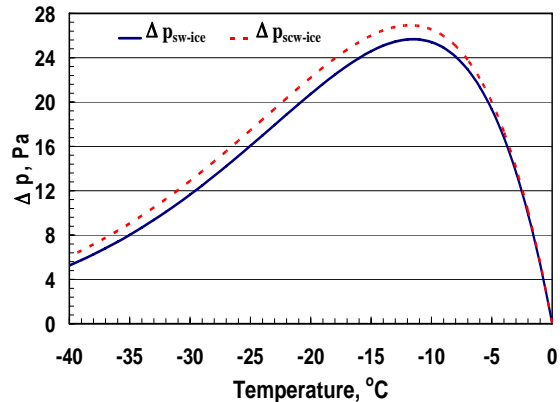


Figure 4: Vapor pressure differences of water and ice, and, super cooled water and ice as function of air dry-bulb temperature.

Thus, driving force of mass transfer toward ice surface is a consequence of ice crystals having lower saturation vapor pressures than liquid droplets do, which creates a gradient of high to low water molecules from liquid to ice that promotes ice growth based on the environmental temperature. This leads to in early stage of frost formation, and this is an enhancement in the rate of mass transfer. As mass transfer process continues, it is assumed that the part of the air water vapor content and all mist droplets in the boundary layer are transported to the frost surface; and freeze at the surface. In addition, diffused water vapor into the existing frost layer before it freezes. Therefore, as time passes, ice crystals on the coil surface join together into larger clumps consisting interlocked aggregates of thin crystals at the surface leading to the ratio ( $UA_{fr}/UA_{dry}$ ) to be around unity. Under this operating condition, both frost thickness and surface temperature increase until frost surface temperature reach to  $0^{\circ}\text{C}$ . Consequently, the frost layer becomes denser and the heat transfer resistance is increased. The mentioned factors decrease heat and mass process through the frost layer. As a result, values of the ratio ( $UA_{fr}/UA_{dry}$ ) are degraded to 0.86. It is worth to mention that the term favorable frost used by Smith [3], Cleland and O'Hagan [8] and Sherif et al. [8] for the frost formed correspondence to psychrometric-sub-saturated region is not generally appropriate. It can be valid only at early stage of frost formation due to the enhancement in both heat transfer and mass transfer process at the evaporator coil surface. Otherwise, frost deposition on cold walls in refrigeration equipments is usually undesirable.

#### 4.2. Case of Frost Formation on Cold Freezer Walls in Psychrometric-Supersaturated Region

The condition of frost formation inside cold storage freezers is different. It is mainly attributable to the infiltration of warm humid air into the freezer. Regarding formed frost inside cold storage freezers, data from the presentation of Simkins [20] is used to investigate demarcation criteria, and to declare whether frost is formed in either psychrometric subsaturated or supersaturated regions and the formed frost characteristics. Data from Simkins [20] on the infiltration air from docking area into the cold storage freezer and the freezer air temperature are plotted in Figure 5. In addition, data is used to calculate demarcation criteria value, which is found Ratio = 3.76. From both the plot and demarcation criterion value, the frost formed on the cold storage freezer walls at this condition is correspondence to psychrometric-supersaturated region. Both the calculated criteria and the plotted data on the psychrometric chart of Figure 5 are completely matched. In addition, it can be recognized for this higher demarcation criteria value. The frost is formed under severe condition. Severe condition for frost formation due to the mixture of infiltration air and freezer air crossing the psychrometric-saturation line at temperature of 4.3 °C, straight-line approach as shown in Figure 5. As the air mixes in a supersaturated region with further cooling with the air fog, and begins to be formed in the mixture followed by formation of ice fog. The ice fog - when presented in the freezer- deposit on any surfaces inside the freezer. Characteristics and shape of ice crystal that forms in the mixed air inside the freezer depend on the environment, temperature and degree of supersaturation condition on psychrometric chart. And is explained as follows. From morphology diagram presented in Libbrecht [19] when air temperature ranges from 0 to -4 °C. Thin plates are formed in psychrometric-subsaturation region and dendrites are formed in psychrometric-supersaturated region. If air temperature ranges from minus four to minus ten °C, columns are formed in subsaturated region and needles are formed in supersaturated region. When air temperature ranges from -10 to -22 °C, plates are formed in subsaturated region and dendrites are formed in supersaturated region. Yet, when the air temperature ranges from -22 to -35 °C, thick plates are formed in subsaturated region and columns are formed in supersaturated region. It can be concluded from the morphology diagram that when air temperature is lowered from 0 to -35 °C, the remarkable sequence of air borne ice crystal habit in psychrometric-supersaturated region. The present case of frost formed inside cold storage is dendrites-needles-dendrites-columns. Şahin [1] stated that whenever a crystal was transferred into a new environment, the continued growth assumed a new habit characteristic of the new conditions. Thus, when needles grown at temperatures between -3 and -5 °C and suddenly moved up in the chamber to about minus two °C, plates develop on their ends. In addition, when similar needles are lowered to about -14 °C, they produce a star shaped crystals. Such radical changes in crystal shape could not be produced by varying the supersaturation at constant temperature. But in some cases they were produced by

only a degree or two changes in temperature at constant supersaturation.

The driving force of mass transfer when air temperature ranges from 0 to -40 °C is shown in Figure 4. As it is explained in previous section- It is higher in the case of saturation vapor pressure difference between super cooled water (fog) and in ice than the saturation vapor pressure difference in case of liquid water and ice at a given temperature. Therefore, when super cooled liquid water drops (fog) and ice particles co-exist in the mixed air inside the cold storage freezer, the liquid maintain a vapor pressure higher than that of the formed ice crystal tolerate. Thus, water vapor deposits on the ice particles surfaces as fast as it evaporates from the water drops. Since the air borne frost is formed in a supersaturated environment, higher mass transfer rate occurs when the mixed air inside the cold storage freezer reach temperature about -12.0 °C. At this temperature, the formed frost has a shape of dendrites that built over needles built over plates, at a temperature ranges from 0 to -10 °C. Moreover, ice crystals continue to grow in this sequence of composite dendrites-needles-dendrites-columns according to air mixed temperature, at expenses of the fog inside the freezer. Whenever, the mixed air reached to the freezer walls and stored products surfaces they deposit on them. The photograph shown in Figure 5 from the presentation of Simkins [20] shows the shape of the frost formed on the surfaces inside the cold storage freezer close to the docks door corresponding to the plotted operating condition.

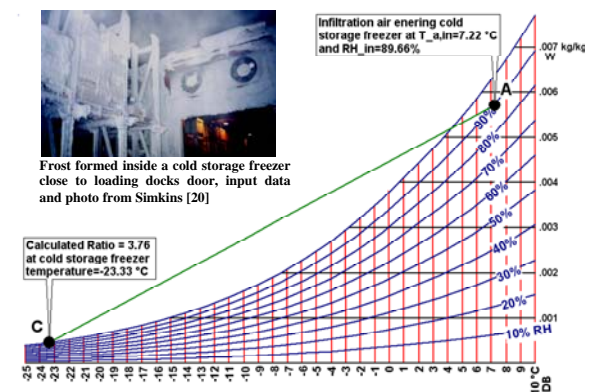


Figure 5: Psychrometric plot of a data from Simkins [20] for infiltration air from dCoking area into the cold storage.

Moreover, additional frost is formed by diffusion of water vapor from high partial vapor pressure conditions in the airstream to lower partial pressures conditions at the deposited frost surface. As shown in Figure 4, the driving force for diffusion of water vapor from high partial vapor pressure conditions in the air stream, either in subsaturation or supersaturation to lower partial pressures conditions at the frost surface is the function of air temperature. It begins at zero value at the triple point, 0.01 °C, and reaches up its maximum value at about -12 °C. In addition, it decreases again as the air temperature decreases. As the cold storage temperature is -23 °C, the diffusion portion from the air to the deposited frost is to be lowered. Consequently, this frost density and thermal conductivity are low, and the deposited frost consists of a porous structure that contains composite structural ice

crystals and air pCokets. This can be recognized from the photograph of Simkins [20] shown in Figure 5.

#### 4.3. Comparison of the Demarcation Criteria Formulas

The only available formula for delineating the demarcation criteria is published by Cleland and O'Hagan [8]. They show that the condition for the demarcation between the frost formed in supersaturated and subsaturated regions is given by the tangent line to the psychrometric saturation curve at the coil surface temperature using the definition of a critical load sensible heat ratio (SHR). They report that, if actual heat loads have a SHR less than critical value, then unfavorable frost is likely to occur, i.e. when the value of  $(SHR_{critical} / SHR_{load})$  is  $> 1.0$ . Their measured operating conditions are shown in Table 4, and are used in this study for validation and comparison of demarcation criteria formulas. Using Cleland and O'Hagan [8] measurement operating conditions as input to the present formula, the calculated criteria values and correspondences demarcation criteria values of Cleland and O'Hagan [8] are presented in Table 4. As shown in Table 4 few cases of demarcation criteria values agree, while most are not. To clarify which formula accurately gives demarcation criteria, plotting few data points in psychrometric chart are shown in Figure 6. The cases in which agreement of general trend of the demarcation criteria calculated by both formulas are the lines (A'-A''), (C'-C'') and (D'-D'') in Figure 6.

The calculated value are sometimes not as the same as shown in Table 4. In some points, Cleland and O'Hagan [8] demarcation criteria indicate that the frost is formed under critical conditions i.e. on border of psychrometric-saturation curve. The graphical plot in this case should be tangent psychrometric-saturation curve. While, when plotting this condition on psychrometric chart line (B'-B'') in Figure 6 as well as the calculated demarcation criteria in this study shown in Table 4 indicates that the condition of frost formation is still in psychrometric-sub-saturated region. Overall, there is no general trend of the differences between both calculated demarcation criteria values by Cleland and O'Hagan Cleland and O'Hagan [8] formula and that calculated values by this study formula, as shown in Table 4. However, as Cleland and O'Hagan [8] reported that although the concept of unfavorable frost is strongly supported, accurate measurement of coil frosting performance is difficult, and the data used here are not of sufficient quality to either fully prove or disprove the proposed transition between frost types. In addition, the calculated demarcation criteria values in this study match very well with the plotted data on the psychrometric chart. Thus, the present developed formula for calculation the demarcation criteria values are able to predict whether the frost is formed on the cold walls at certain operating condition is corresponding to either psychrometric-sub-saturated or supersaturated region precisely.

## 5. Conclusions

A new direct formula predicting demarcation boundaries in psychrometric saturation for delineation the frost formation on cold walls is presented. The formula uses data of the entering air dry-bulb temperature, absolute humidity, the absolute humidity of air at saturation correspondence to the coil surface temperature.

TABLE 4: Comparison of the present results for the demarcation criteria with results of Cleland and O'Hagan [8]

Operating conditions of Cleland and O'Hagan (2003)			Demarcation criteria of Cleland and O'Hagan [8]	Demarcation criteria of the Present study	Plotted line in Fig. (6)
$T_{a,in,Co}$	$RH_{in,Co}$ %	$T_{ref,Co}$			
-0.2	68	-9	0.93	0.57	
-0.4	68	-9.7	0.94	0.62	A'-A''
-1.6	72	-11.6	1	0.8	B'-B''
-0.8	83	-9.7	1	1	C'-C''
-1.6	82	-10.1	1.03	0.94	
-0.3	82	-8.4	1	0.9	
0.0	76	-10.5	1.06	0.94	
0.2	77	-10	1.04	0.93	
-0.6	78	-11.4	1.06	1.02	
-0.4	81	-10.2	1.01	1.01	
-1.4	87	-10.4	1	1.12	
-0.7	89	-8.9	1.06	1.11	
-1.8	87	-11.2	1.13	1.15	
-0.1	87	-9.1	1.17	1.11	
0.1	93	-10.5	1.17	1.39	
0.2	93	-10.6	1.17	1.41	D'-D''

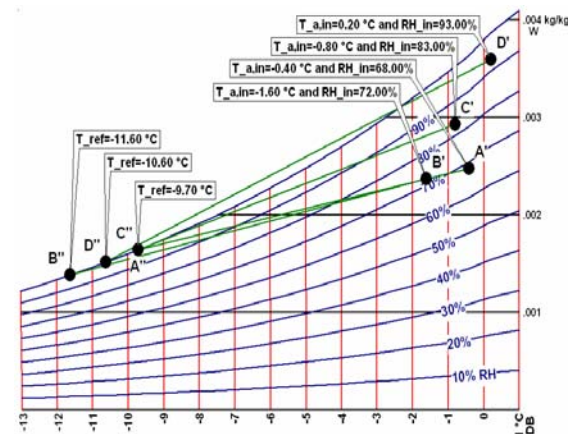


Figure 6: Psychrometric plot of data from Cleland and O'Hagan [8] to declare the demarcation criteria conditions.

The developed formula predicts either frost formation is in psychrometric-sub-saturated or is in supersaturated region on the cold walls precisely. Case studies of demarcation criteria for frost formation on evaporator coil using experimental measured data and on walls of cold storage freezer using measured data from literature are used to validate the formula. The results of these studies are summarized as follows:

- The calculated demarcation criteria values in this study are complete when matched with the plotted data using the psychrometric chart. Therefore, the developed formula for calculation of the demarcation criteria values is able to predict whether the frost is formed on the cold walls at certain operating condition is corresponding to either psychrometric-sub-saturated or supersaturated region.

- For an evaporator coil working at higher freezing temperature, the demarcation criteria is guided to interpret the enhancement in heat transfer and mass transfer coefficients at the operating condition. The characteristic of the frost formed on the coil under aforementioned condition was found to be thin, fluffy, and dryer. This declares that the type and shape of frost crystal forms on the coil surface reflect growth environment.
- In case of cold storage freezers, clearly a higher value of demarcation criteria is an indication that the frost is formed under severe condition. In such case, as the frost is formed corresponds to psychrometric-supersaturated region under severe condition. Its crystal composite of dendrites-needles-dendrites-columns is based on the environmental in the freezer.
- The term favorable frost used in the literature for the frost formed corresponding to psychrometric-sub saturated region is not generally appropriate. It can be valid only at early stage of frost formation due to the enhancement in both heat transfer and mass transfer coefficients at the evaporator coil surface. Otherwise, frost deposition on cold walls in refrigeration equipments is usually undesirable.

## REFERENCES

- [1] Şahin, A.Z., "An analytical study of frost nucleation and growth during the crystal growth period". Heat and Mass Transfer, Vol. 30, 1995, 321-330.
- [2] Dietenberger, M.A., "A Frost Formation Model and Its Validation under Various Experimental Conditions". NASA Contractor Report No.3595, 1982, 68p.
- [3] Smith, G.R., "Theoretical cooling coil calculations at freezer temperatures to avoid unfavourable coil frost". ASHRAE Transactions, Vol. 95 (2), 1989, 1138-1148.
- [4] Smith, G.R., "Latent heat, equipment-related load, and applied psychrometrics at freezer temperatures". ASHRAE Transactions, Vol. 98 (2), 1992, 649-657.
- [5] Smith, G.R., "Coil icing and other opportunities within freezer/anteroom complexes". ASHRAE Transactions, Vol. 112 (2), 2006, 469-484.
- [6] Sherif, S.A., Mago, P., Al-Mutawa, N.K., Theen, R.S., Bilen, K., "Psychrometrics in the supersaturated frost zone". ASHRAE Transactions, Vol.107 (2), 2001, 753-767.
- [7] Mago, P.J. and Sherif, S.A., "Modeling the cooling path of a dehumidifying coil under frosting conditions". ASME J of Heat Transfer, Vol. 124, 2002, 1182-1191.
- [8] Cleland, D.J. and O'Hagan, A.N., "Performance of an air-cooling coil under frosting conditions". ASHRAE Transactions, Vol. 109 (2), 2003, 243-250.
- [9] Cleland, D.J., "Implications of coil frosting on systems design for low temperature applications". ASHRAE Transactions, Vol. 111 (1), 2005, 336-345.
- [10] Cleland, D.J., "Cold store and loading design to minimize condensation and coil frosting problems". In CD of the International Congress of Refrigeration, Beijing, 2007, Paper No. ICR07-D1-409.
- [11] Stoecker, W.F., "Industrial Refrigeration Handbook". Business News Publishing Company, Michigan, 1988.
- [12] ASHRAE, 2004 "ASHRAE Handbook - Systems and Equipment", ch.S21 SI. American Society of Heating, Refrigerating and Air-Conditioning Engineers. Atlanta, Georgia, 2004.
- [13] ASHRAE, 2005 "ASHRAE Handbook - Fundamental", ch.F06 SI. American Society of Heating, Refrigerating and Air-Conditioning Engineers. Atlanta, Georgia, 2005.
- [14] Magnus, G., "Versuche über die Spannkraft des Wasserdampfes". Annalen der Physik und Chemie, Vol. 61 No.2, 1844, 225-248.
- [15] Sonntag, D., "New values for the thermodynamic parameters of water vapor". Izmeritel'naya Tekhnika, Vol. 9, 1982, 54-56.
- [16] WMO, "Measurement of Humidity", 2006, ch.4, In, Guide to Meteorological Instruments and Methods of Observation. Preliminary seventh edition. Geneva - Switzerland.
- [17] Whiteman, C.D., De Wekker, S.F.J., and Haiden, T., "Effect of dewfall and frostfall on nighttime cooling in a small, closed basin". J. of Applied Meteorology and Climatology, Vol. 46, 2007, 3-13.
- [18] [Ali, Ahmed Hamza H. and Ismail, Ibrahim M. "Evaporator airside fouling: Effect on performance of room air conditioners and impact on indoor air quality". Int J of HVAC&R Research, Vol. 14 No.2, 2008, 209-219.
- [19] Libbrecht, K.G., "Morphogenesis on ice: The physics of snow crystals". Engineering & Science, Vol. 64, No.1, 2001, 10-19.
- [20] Simkins, B., "Dehumidification approaches for cold storage loading design". Presentation at ASHRAE Winter Meeting, Atlanta, GA, 2001.